

Supplementary Information

An *in situ* investigation of the water-induced phase transformation of USTA-74 to MOF-74(Zn)

Bart Bueken,^a Helge Reinsch,^b Niclas Heidenreich,^b Annelies Vandekerkhove,^a Frederik Vermoortele,^a Christine E. A. Kirschhock,^a Norbert Stock,^b Dirk De Vos^a and Rob Ameloot^{a,*}

^a Centre for Surface Chemistry and Catalysis, Department M²S, KU Leuven, Celestijnenlaan 200F p.o. box 2461, 3001 Leuven, Belgium

^b Institut für Anorganische Chemie, Christian-Albrechts Universität zu Kiel, Max-Eyth Straße 2, D-24118 Kiel, Germany.

Table of Contents

Experimental procedures	3
Synthesis of UTSA-74 and transformation to MOF-74(Zn)	3
Materials characterization	3
Synchrotron experiments	5
Optical images of UTSA-74 crystals	6
Single crystal X-ray diffraction of UTSA-74	7
Fourier transform infrared spectroscopy	8
Thermogravimetric analyses	9
CO ₂ physisorption	10
Stability in organic solvents	11
Phase transformation in water	12
References	17

Experimental procedures

Synthesis of UTSA-74 and transformation to MOF-74(Zn)

All chemicals used in the synthesis of UTSA-74 were commercially obtained from TCI Europe N.V. and Acros Organics and used without further purification.

In a representative synthesis, 4.5 mmol of $\text{Zn}_2(\text{CH}_3\text{COO})_4 \cdot 2\text{H}_2\text{O}$ (1 g) and 2.5 mmol of 2,5-dihydroxy-1,4-benzenedicarboxylic acid (0.5 g) were dissolved in 50 ml of dimethyl sulfoxide (DMSO) and placed in a 100 ml glass screw cap bottle. After closing, the reaction vessel was placed in a preheated conventional synthesis oven at 110 °C for 72h. After reaction, yellow hexagonal single crystals of UTSA-74 could be isolated by decanting the spent synthesis liquor. The synthesis of UTSA-74 could easily be scaled to 250 ml of DMSO. To remove guest molecules from the pores, UTSA-74 crystals were soaked five times in ethanol at 80 °C overnight, and dried at 80 °C.

Transformation of UTSA-74 to MOF-74(Zn) was performed using ethanol-exchanged single crystals of UTSA-74, which were suspended in a certain volume of deionized water. For the *in situ* synchrotron X-ray diffraction experiments, 100 mg of UTSA-74 was suspended in 3 ml water, and heated to the desired temperature under stirring (*vide infra*). For the in-house *in situ* experiment, a 1 mm borosilicate glass capillary (Hilgenberg nr. 14) was loaded with 10 mg of UTSA-74. Water was subsequently carefully injected using a syringe, to avoid the formation of air bubbles, until the capillary was 3/4th filled with an UTSA-74 slurry. The capillary was immediately flame-sealed and diffraction data was recorded at ambient temperature. The static transformation under water vapour was performed by loading a 1.2 ml glass vial with 20 mg of UTSA-74, placing this vial in a larger, sealed 10 ml vial containing 1.5 ml water, and placing this in a conventional synthesis oven at 60 °C. Scanning electron micrographs were recorded *ex situ* at various stages of the static transformation reaction performed on 30 mg MOF suspended in 3 ml of water at 50 °C. After full conversion to MOF-74(Zn), similar samples were used to determine the porosity of the formed MOF-74(Zn).

Materials characterization

X-ray diffraction

To confirm the synthesis of UTSA-74, single crystal X-ray data was collected on a suitable ethanol-exchanged single crystal using an Agilent Supernova diffractometer, equipped with an Atlas CCD detector (Mo K_α radiation, $\lambda = 0.71073$ Å, graphite monochromator) at 293 K. The images were interpreted and integrated using the CrysAlisPro software (Agilent Technologies).¹ The structure was solved with the

ShelxS-97 structure solution program using Direct Methods and refined with the ShelxL-97 refinement package using full-matrix least squares minimization on F^2 .² Disordered electron density attributed to the guests in the pores was approximated by oxygen atoms.

High resolution powder X-ray diffraction patterns were recorded on UTSA-74 and MOF-74(Zn) samples packed in 0.7 mm borosilicate glass capillaries, which were mounted on a STOE Stadi MP diffractometer with focusing Ge(111) monochromator (Cu $K_{\alpha 1}$ radiation, $\lambda = 1.54056 \text{ \AA}$) in Debye-Scherrer geometry and equipped with a linear position sensitive detector (PSD; $6^\circ 2\theta$ window; $0.01^\circ 2\theta$ resolution). Patterns were recorded at room temperature in the range $1 - 90^\circ 2\theta$ with step width of $0.5^\circ 2\theta$ and a step time of 50 s. The samples were continuously rotated to improve statistics and eight diffraction patterns were recorded. All eight were found to be nearly identical and thus merged to improve the signal to noise ratio.

High-throughput powder X-ray diffraction patterns were recorded on a STOE COMBI P diffractometer (monochromated Cu $K_{\alpha 1}$ radiation, $\lambda = 1.54060 \text{ \AA}$) equipped with an IP-PSD detector in transmission geometry.

General characterization

Scanning electron microscopy (SEM) micrographs were recorded using a JEOL-6010LV SEM after depositing a palladium/gold layer on the samples using a JEOL JFC-1300 autofine coater under Ar plasma.

Thermogravimetric analyses were performed on a TA instruments TGA Q500. Samples were heated at a rate of $5^\circ\text{C}\cdot\text{min}^{-1}$ to 700°C under an O_2 flow.

Fourier transform infrared (FTIR) spectra were recorded on a NICOLET 6700 spectrometer (Thermo-Fischer) within the $500 \text{ cm}^{-1} - 4000 \text{ cm}^{-1}$ range (256 scans; 2 cm^{-1} resolution). UTSA-74 Samples were analysed as a pressed wafer of 5 wt% MOF in KBr. Spectra were recorded at 100°C to remove physisorbed water from the samples.

N_2 physisorption measurements were performed on a Micromeritics 3Flex surface analyzer at liquid nitrogen temperature (77 K). Prior to the measurements, the samples (50-100 mg) were outgassed for 6h at 150°C and 0.1 mbar vacuum. Surface areas were calculated using the multi-point BET (Brunauer-Emmett-Teller) method applied to the isotherm adsorption branch, in line with the Rouquerol consistency criteria.³

A CO_2 physisorption isotherm was measured on 75 mg of UTSA-74, outgassed overnight at 150°C and 0.1 mbar vacuum, using a Micromeritics ASAP 2420 instrument, at 298 K in the $1 - 1000 \text{ mbar}$ pressure range.

Synchrotron experiments

All experiments were carried out in a custom-built *in situ* cell constructed for synchrotron experiments. The set-up is described in more detail elsewhere.⁴ Briefly described the cell consists of a Pyrex glass reactor which is placed inside a heating mantle. The complete device also comprises a magnetic stirrer and a compressed air cooling system. Moreover, a syringe pump can be connected to the reactor to dose reactants during the experiment. For our purposes the reactor was equipped with a magnetic stirring bar, 3 ml of H₂O and 100 mg of UTSA-74 crystals, and swiftly placed inside the heating mantle, which was subsequently rapidly heated to the respective temperature. *In situ* time-resolved powder X-ray diffraction experiments were carried out at 110 °C and 120 °C, respectively, with a temporal resolution of 30 seconds. All experiments were carried out at beamlines P08⁵ or P09⁶ at DESY (Hamburg) using a monochromated beam with a wavelength of 0.51662 Å (beamline P08) or 0.53905 Å (beamline P09). Data was collected using a two-dimensional Perkin Elmer 1621 detector (resolution 2048 x 2048 pixel). The detector position was determined and the set-up calibrated using CeO₂ as standard with the software Fit2D.⁷ The data were integrated and normalised based on the strongest reflection originating from the aluminium plate of the heating mantle to account for beam intensity fluctuations. The integral of the strongest reflection, for UTSA-74 and MOF-74(Zn) corresponding to the (2¹0) plane, was considered proportional to the amount of MOF in suspension, and integrated using the F3 software tool.⁸ The peak integrals were checked for consistency and in case the peak profile was not well fit the values were ignored or set to 0 when no peak was visible. The normalised value of this integral was therefore plotted as reaction progress α as a function of reaction time t .

Optical images of UTSA-74 crystals

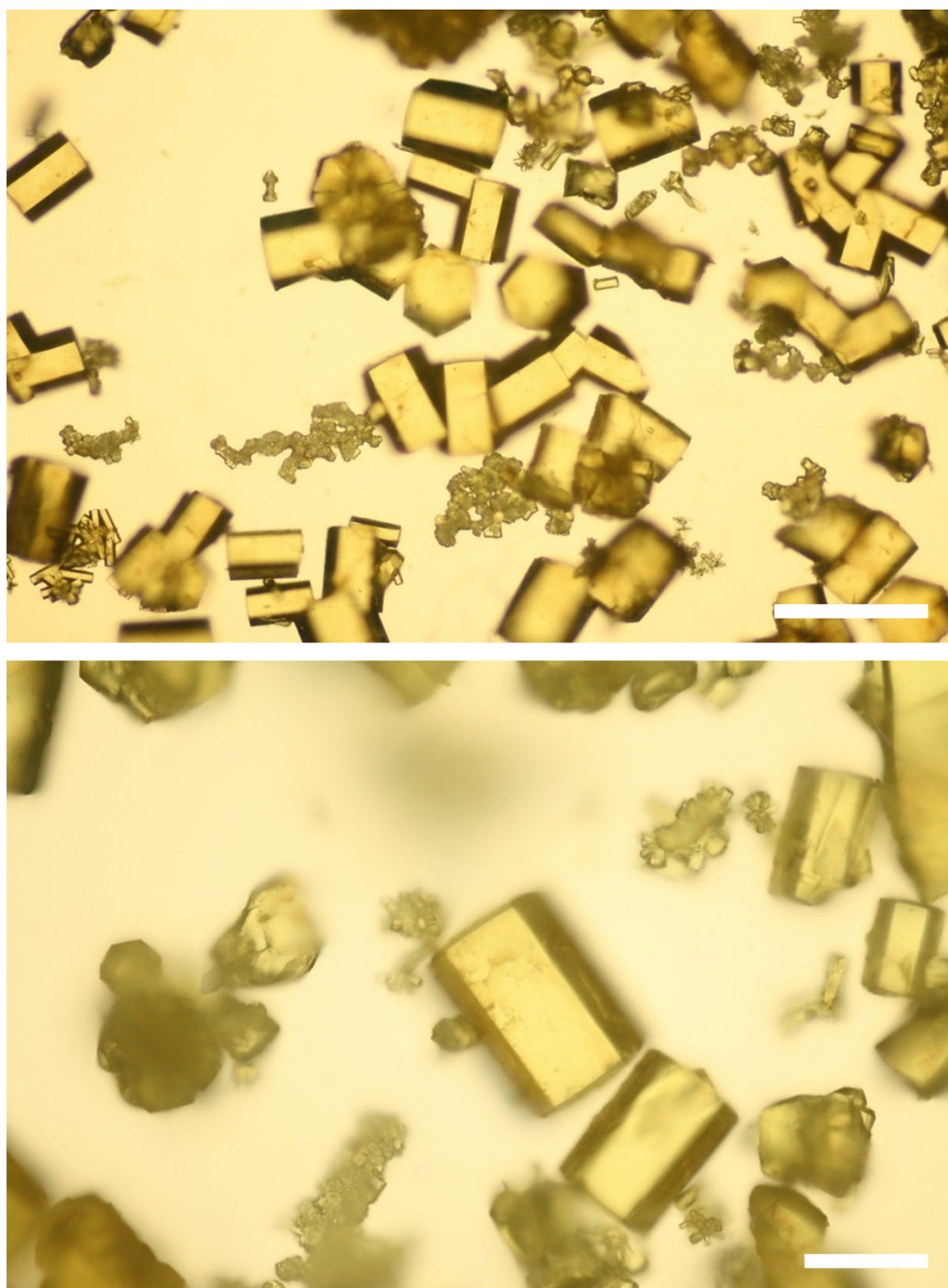


Fig. S1. Optical images of as-synthesized hexagonal single crystals of UTSA-74 of various sizes. Powder X-ray diffraction provided no indication for the presence of MOF-74(Zn) in these as-synthesized samples. Top: scale bar = 200 μm ; bottom: scale bar = 100 μm .

Single crystal X-ray diffraction of UTSA-74

Table S1. Crystallographic data for UTSA-74 determined from laboratory single crystal X-ray diffraction data recorded from an ethanol-exchanged single crystal.

Formula	C ₄ O _{5.37} Zn
<i>M</i> / g·mol ⁻¹	199.36
Space group	<i>R</i> ³ <i>c</i> (n° 167)
<i>a</i> / Å	22.939(3)
<i>b</i> / Å	22.939(3)
<i>c</i> / Å	15.8638(13)
α / °	90.00
β / °	90.00
γ / °	120.00
<i>V</i> / Å ³	7229.2(15)
<i>Z</i>	36
<i>T</i> / K	293
<i>F</i> (000)	3491
μ (Mo K α) / mm ⁻¹	3.028
Reflections measured	10003
Unique reflections	1647
Goodness of Fit	1.172
<i>R</i> (int)	0.0923
<i>wR</i> ₂ (all data)	0.2120

Fourier transform infrared spectroscopy

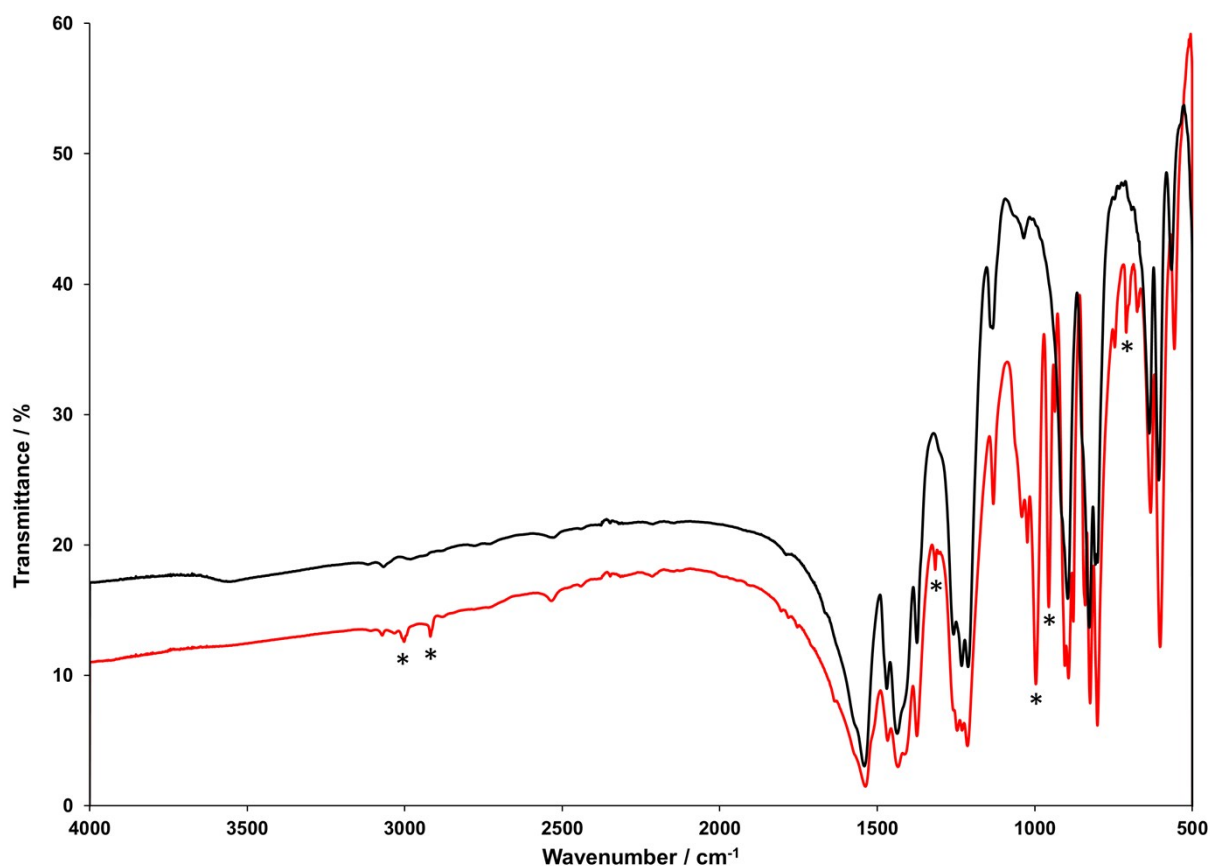


Fig. S2. Fourier transform infrared spectra (FTIR) of as-synthesized UTSA-74 (red) and evacuated UTSA-74 (black). Spectra were recorded on pressed KBr wafers containing 5 wt% MOF (128 scans, 2 cm⁻¹ resolution) at 100 °C to evacuate water from the wafers. Vibrational bands associated with dimethyl sulfoxide present in as-synthesized UTSA-74 are highlighted with an asterisk.

Thermogravimetric analyses

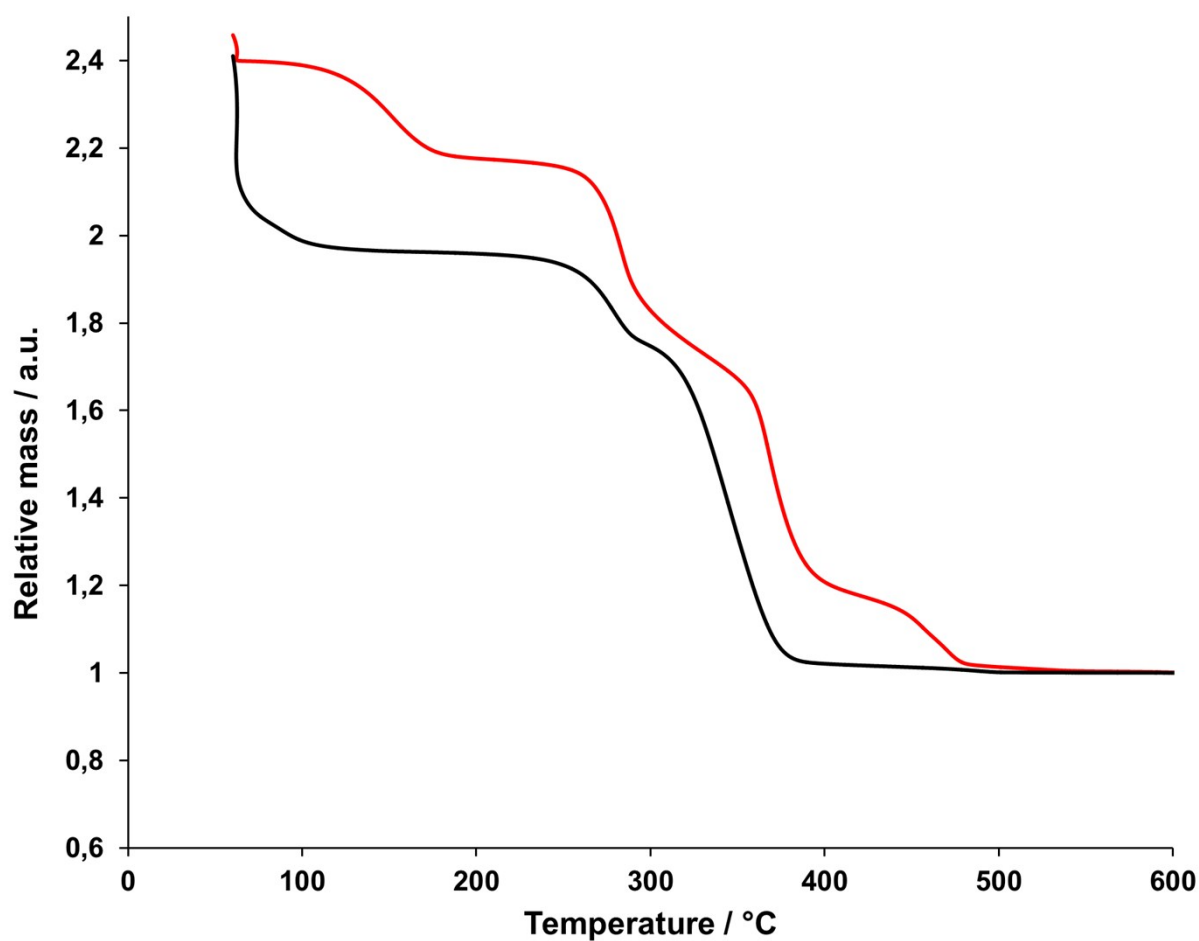


Fig. S3. Thermogravimetric analyses of as-synthesized UTSA-74 (red) and evacuated UTSA-74 (black) measured under an O₂ atmosphere at a ramp rate of 5 °C·min⁻¹. The initial mass loss of the latter can be attributed to atmospheric water adsorbed prior to the measurement.

CO₂ physisorption

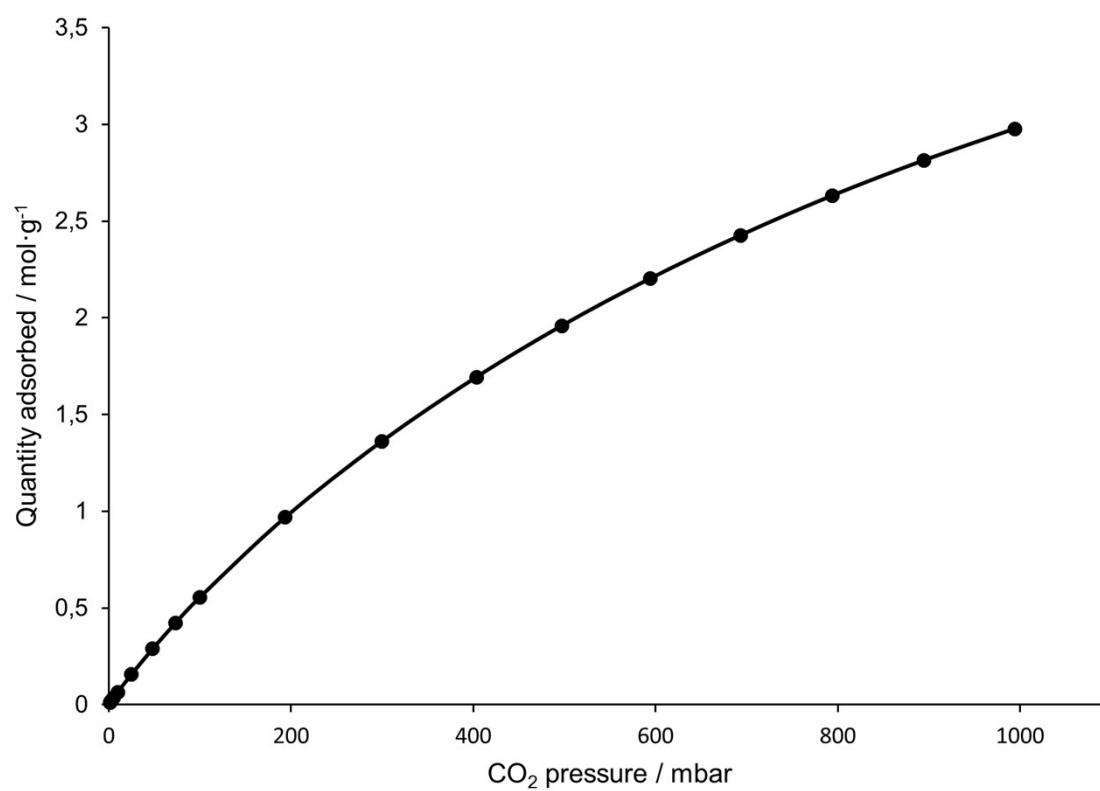


Fig. S4. CO₂ physisorption isotherm for UTSA-74 (298 K).

Stability in organic solvents

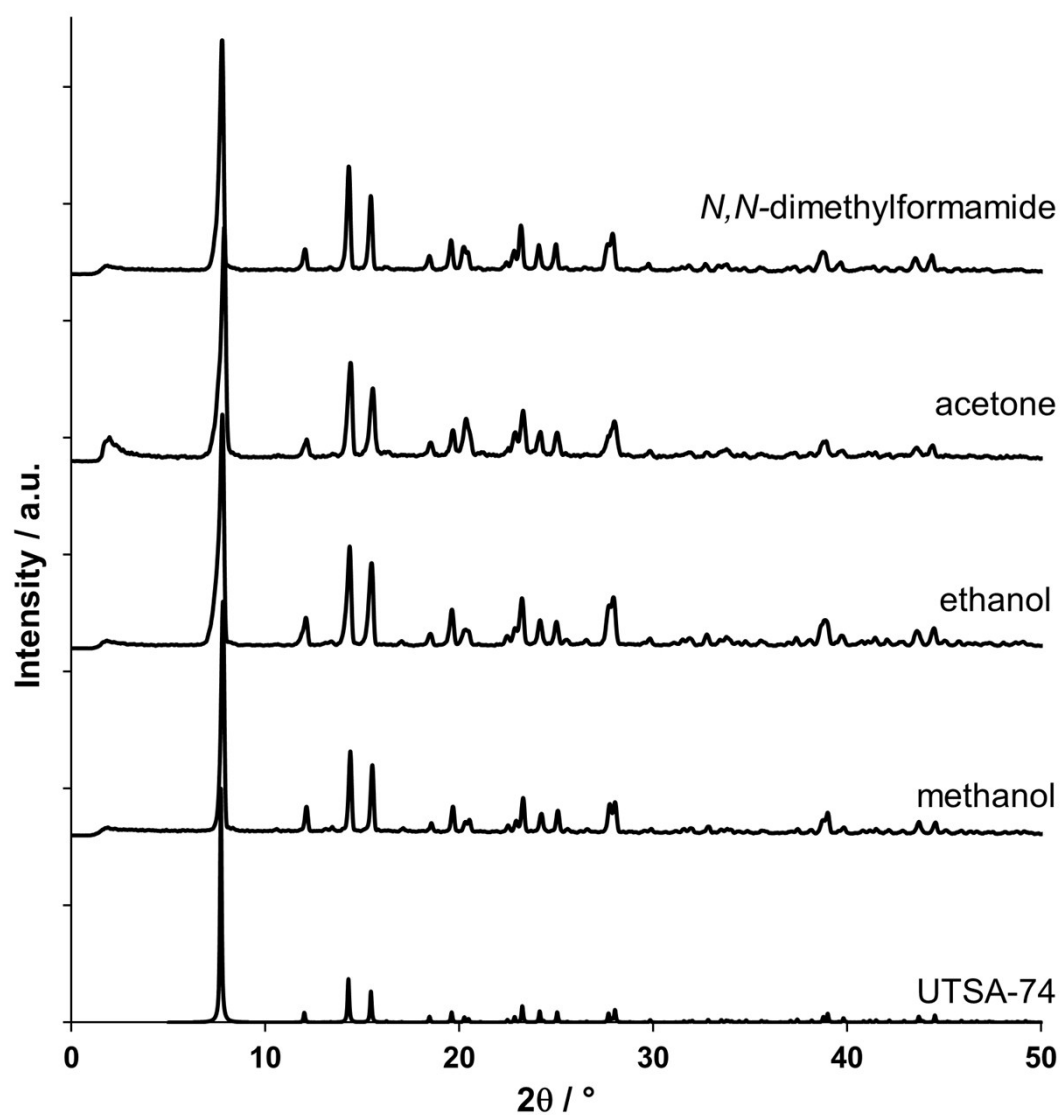


Fig. S5. Powder X-ray diffraction patterns of UTSA-74 immersed in various solvents for 72h at room temperature, indicating the stability of the material in these conditions.

Phase transformation in water

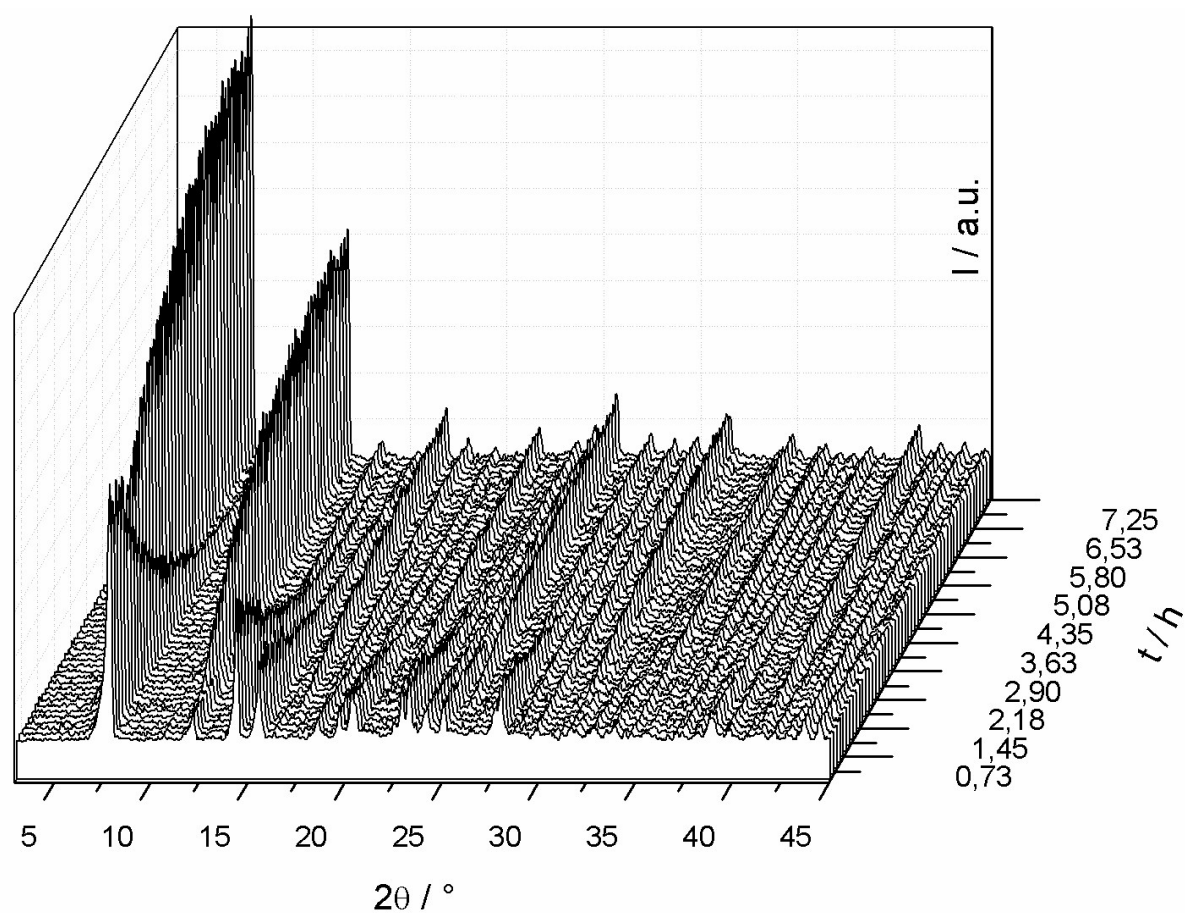


Fig. S6. Time-resolved *in situ* powder X-ray diffraction patterns of the UTSA-74 to MOF-74(Zn) phase transformation at 298 K under static conditions. For the experiment, a 1 mm glass capillary was filled with 10 mg of ethanol-exchanged UTSA-74, deionized water, sealed and immediately loaded into the diffractometer.

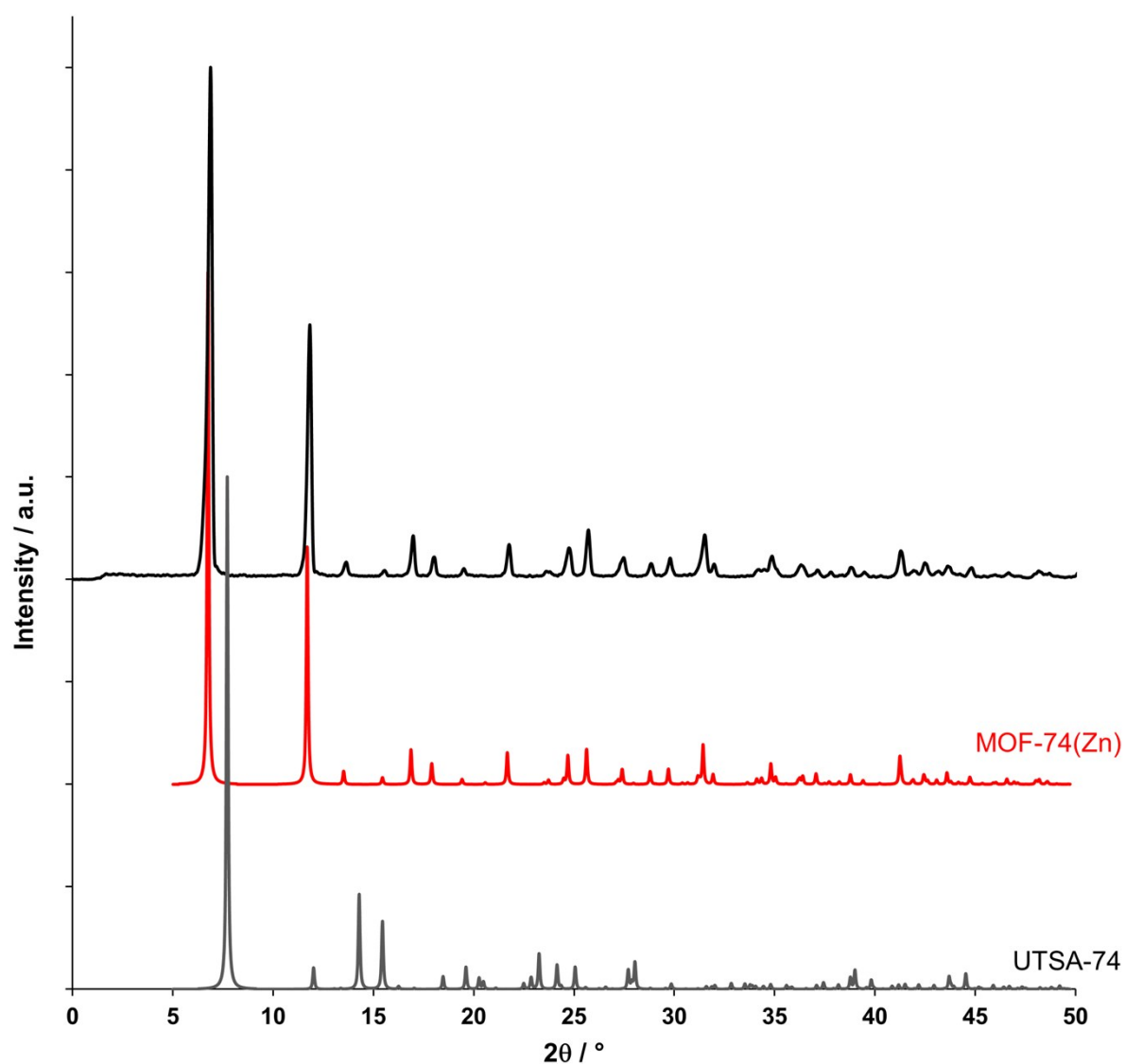


Fig. S7. Powder X-ray diffraction pattern of UTSA-74 exposed to water vapour at 60 °C for 14 days (black), with a full conversion to hydrated MOF-74(Zn). The theoretical diffraction patterns for hydrated MOF-74(Zn) and UTSA-74 are provided in red and grey, respectively.⁹

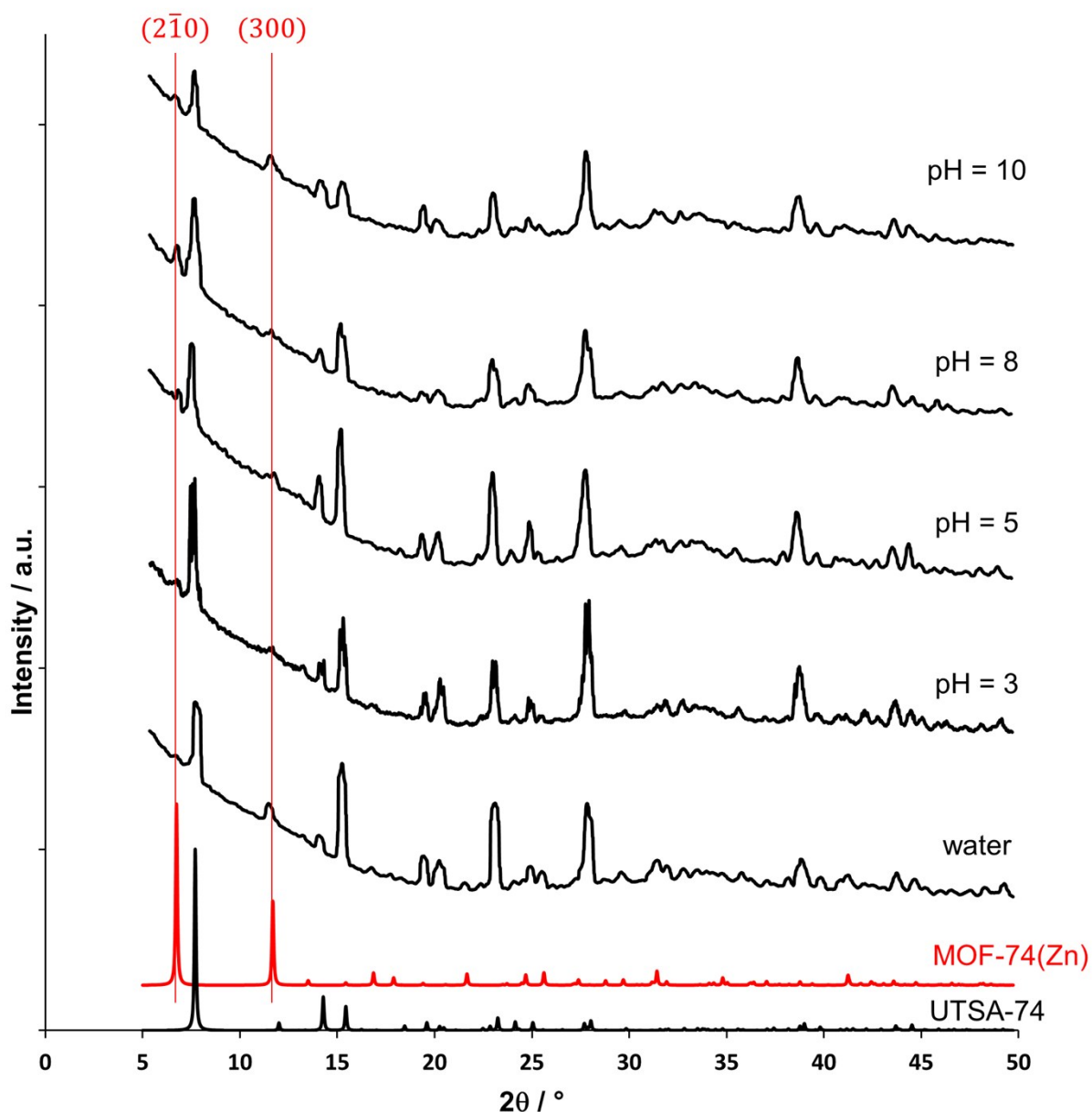


Fig. S8. Powder X-ray diffraction patterns extracted from the original report of Luo *et al.*¹⁰ for UTSA-74 immersed in water at various pH for 24 h. A partial conversion to MOF-74(Zn) can be observed in all patterns, as indicated by the appearance of the highlighted $(2\bar{1}0)$ and (300) reflections of MOF-74(Zn).⁹ No direct comparison could be made to our experiments, as no additional experimental procedures were reported by Luo *et al.*

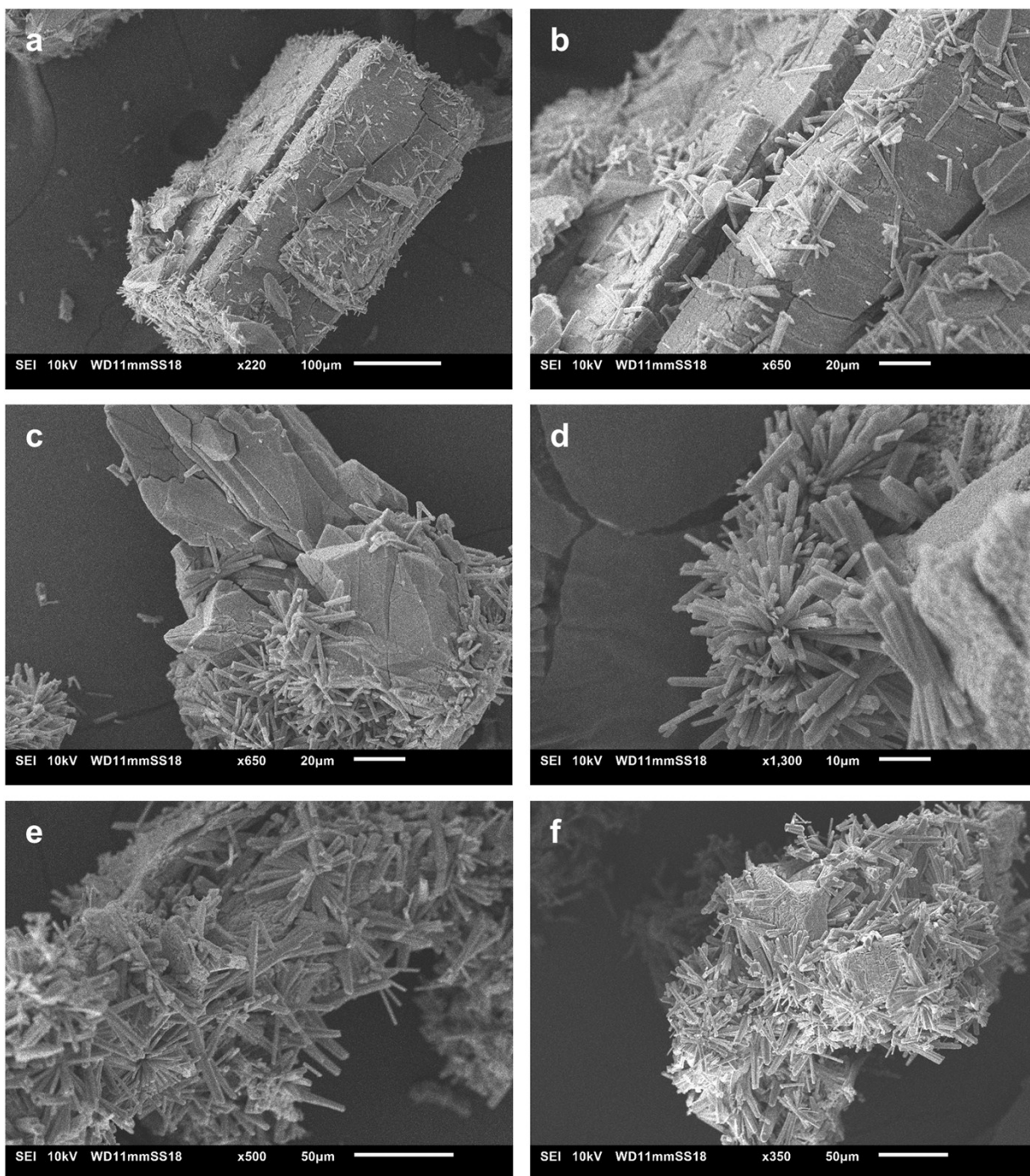


Fig. S9. Scanning electron micrographs recorded at various stages of the UTSA-74 to MOF-74(Zn) transformation at 50 °C under static conditions. (a) A large UTSA-74 crystal, with needle-like crystals of MOF-74(Zn) growing on its surface (1h reaction). (b) Close-up of (a), showing cracks on the surface of the UTSA-74 crystal. (c) UTSA-74 crystal fragment, with MOF-74(Zn) crystals (1h reaction). (d) Close-up of (c), showing how UTSA-74 adopts a sponge-like texture during dissolution. (e-f) MOF-74(Zn) crystals growing on decomposing fragments of UTSA-74 (2h reaction).

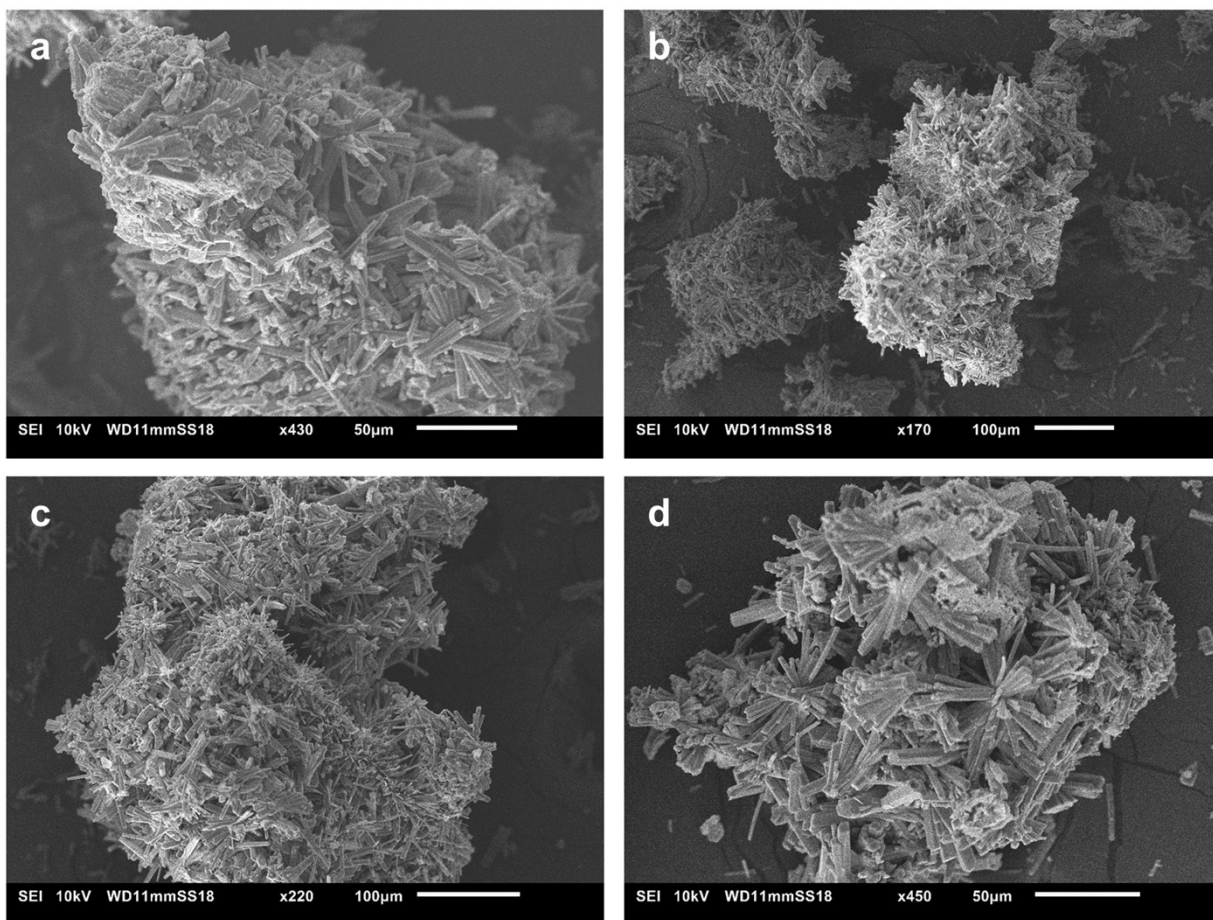


Fig. S10. Scanning electron micrographs recorded at various stages of the UTSA-74 to MOF-74(Zn) transformation at 50 °C. (a-b) Extensive growth of MOF-74(Zn) crystals (3h reaction). (c-d) Near-full conversion of UTSA-74 to MOF-74(Zn) (4h reaction).

References

1. CrysAlis Pro. Agilent Technologies Ltd., Yarnton, United Kingdom. 2012.
2. G. M. Sheldrick, *Acta Crystallogr. Sect. A Found. Crystallogr.*, 2008, **64**, 112–122.
3. J. Rouquerol, F. Rouquerol, and K. S. W. Sing, *Absorption by Powders and Porous Solids*, 1998.
4. H. Reinsch, J. Benecke, M. Etter, N. Heidenreich, and N. Stock, *Dalt. Trans.*, 2017, **46**, 1397-1405.
5. O. H. Seeck, C. Deiter, K. Pflaum, F. Bertam, A. Beerlink, H. Franz, J. Horbach, H. Schulte-Schrepping, B. M. Murphy, M. Greve and O. Magnussen, *J. Synchrotron Rad.*, 2012, **19**, 30–38.
6. J. Stremper, S. Francoual, D. Reuther, D. K. Shukla, A. Skaugen, H. Schulte-Schrepping, T. Kracht and H. Franz, *J. Synchrotron Rad.*, 2013, **20**, 541–549.
7. A. P. Hammersley, S. O. Svensson, M. Hanfland, A. N. Fitch, and D. Hausermann, *High Press. Res.*, 1996, **14**, 235–248.
8. F3 software tool. A. Rothkirch, Hamburg, 2010.
9. P. D. C. Dietzel, R. E. Johnsen, R. Blom, and H. Fjellvåg, *Chem. - A Eur. J.*, 2008, **14**, 2389–2397.
10. F. Luo, C. Yan, L. Dang, R. Krishna, W. Zhou, H. Wu, X. Dong, Y. Han, T.-L. Hu, M. O’Keeffe, L. Wang, M. Luo, R.-B. Lin, and B. Chen, *J. Am. Chem. Soc.*, 2016, **138**, 5678–5684.